Design, Synthesis, Antimicrobial, Cyclic Voltammetry and Molecular Docking Studies of L-Methionine founded Schiff bases

Marulasiddeshwara M. B.[1*], Dakshayani S. S.[2], Somashekar M. N.[3], Satheesh C. E.[4], Golla Ramesh[4], Shivaraja G.[5], P. Raghavendra Kumar[4*]

{ mbmsiddesh@gmail.com[1*], somu.smn@gmail.com[3], sathesh.in@gmail.com[4], rameshap111@gmail.com[4], shivaraj274aras@gmail.com[5], raghukp1@gmail.com[4*] }

[1]Department of Studies and Research in Organic Chemistry, Janasiri Campus, Tumkur University, Bidarakatte, Karnataka - 572118, Karnataka, India
[2]Department of Biotechnology, UCS, Tumkur University, Tumkur-572103, Karnataka, India
[3]Department of Chemistry, Shri Prabhu Arts, Science and J M Bohra Commerce Degree College, Shorapur, Yadgiri District. Karnataka-585224, India
[4]Department of Studies and Research in Chemistry, Tumkur University, Tumkur-572103, Karnataka, India
[5]Department of Chemistry, Srinivas University, Mukka, Mangaluru-574146, Dakshina Kannada, Karnataka, India

Abstract. By condensing L-2-amino-4-methylthio derived amide, **2** with substituted aldehydes, 5-chloro salicylaldehyde, 5-bromo salicylaldehyde, and orthovanillin resulted a new chiral Schiff bases, **3a-3c**. using CHN analysis, polarimetry, spectroscopic studies. The synthesized Schiff bases have been characterised. The antimicrobial assessment of all of the Schiff bases against pathogenic microbial strains proved large antibacterial and antifungal activity with sturdy growth inhibition. The insilico docking studies of Schiff bases inside the active website online of DNA Gyrase (PDB: 3G75) found out favorable binding energies starting from -6.07 to - 7.59 kcal/mol. Additionally, docking with N-Myristoyltransferase (PDB: 1IYL) showed even more potent interactions, with binding energies among -8.9 and -10.2 kcal/mol.

Keywords: Synthesis**,** Schiff base, Antimicrobial, Molecular Docking Studies

FPCS 2024, November 13-14, Bengaluru, India

DOI 10.4108/eai.13-11-2024.2355666

1 Introduction

Amino acids and polypeptides serve as essential structural components of living things. These compounds done Schiff base development gives them antithrombotic characteristics. Amino acid-derived peptide Schiff bases have vital biological roles. Amino acids are the building blocks of life and served as units in the proteins. Many activities, including neurotransmitter transport and biosynthesis, are complicated by amino acids. Unnatural analogs have become more prevalent in molecules in recent years, particularly in those that may have medicinal applications. [1-5]

A dimethyl derivative of dopamine (DA), 2-(3,4-dimethoxyphenyl) ethanamine is a crucial precursor for several neurotransmitter agents and necessary biomolecules. The emergence of behaviors associated with anxiety is connected to the activation of dopamine (DA) and its derivatives by stress. Clinical findings raised the possibility that DA malfunction plays a role in social anxiety disorder [6-9].

Schiff bases combine two aromatic/heterocyclic physiologically active groups with an azomethine (C=N) linkage, which results in a variety of molecular mixtures with fascinating biological features. Schiff bases are useful medicinal agents since they can association with different metals to generate stable complexes [10-14].

Owing to the abovementioned facts we herein reported the synthesis, cyclic voltammetry, molecular docking and antimicrobial studies of new amino acid amide derived Schiff bases **3a-3c** are reported by treating L-2-amino-N-(3,4-dimethoxyphenethyl)-4-(methylthio)butanamide (**2**) with various salicylaldehyde derivatives such as 5-chloro salicylaldehyde, 5-Bromo salicylaldehyde and ortho vanillin. All the produced Schiff bases were structurally categorized by elemental analysis, polarimetry, and spectroscopic studies.

2. Experimental

2.1 Materials and methods

Boc-L-methionine, orthovanillin, 5-chlorosalicylaldehyde, and 5-bromosalicylaldehyde have been acquired and used without equally purification. The reactions have been monitored by means of thin-layer chromatography (TLC). Uncorrected melting points have been decided using a RAGA melting point equipment in open capillaries. Elemental composition became analyzed using a LECO–CHNSO–9320 kind elemental analyzer, at the same time as UV-seen absorption statistics had been collected with an Agilent Cary-60 spectrophotometer. ^{1}H- and ^{13}C{1H}-NMR spectra have been recorded the usage of Agilent VNMRS-four hundred and Bruker WM-400 400MHz NMR spectrophotometers, with tetramethylsilane (TMS) as an inner standard. At the same time, cyclic voltammetry became accomplished in CH_3CN with zero.1M $^{t}Bu_4NPF_6$ as assisting electrolyte. The microbial interest changed into assessed through the microdilution approach. The use of Biosolve IT and GOLD 5.1, Insilico studies were conducted at the Schiff base compounds.

2.2 Procedure for the preparation of Chiral Schiff bases (3a-3c).

L-2-amino-N-(three,4-dimethoxyphenethyl)-4-(methylthio)butanamide (**2**) (1.0 mmol) changed into inspired in 20 mL dry methanol at lab temperature for 30 minutes before adding 5-chloro salicylaldehyde (1 mmol), 5-Bromo salicylaldehyde (1 mmol), and ortho vanillin (1 mmol) in 20 mL of dry methanol dropwise with stirring. 10 mL n-hexane became used twice for washing the yellow precipitate, which turned into then vacuum-dried. The reaction's development was determined through TLC. The rotary evaporator turned into used to concentrate the reaction solution resulted a yellow solid of **3a-3c**.

3a: Yield: 355 mg (90%); m.p.80-81°C; Elemental Anal. calcd. (found) for $C_{22}H_{27}N_2O_4SCl$: C, 58.59 (58.60); H, 6.03 (6.05); N, 6.21 (6.27); FT-IR (ATR, ν cm^{-1}): 3333, 2934, 2833, 1648, 1629, 1544, 1512, 1257, 1230, 1137, 1026, 811, 639; UV-Vis (λ_{max} nm, ε $M^{-1}cm^{-1}$): 330, 435; ^{1}H NMR (399.82MHz, chloroform-d, δ ppm): 12.272 (s, 1H, OH), 8.280 (s, 1H, CH=N), 7.317-7.339 (d, 1H, H14), 7.273 (bs, 1H, H17), 6.937-6.959 (d, 1H, H15), 6.638-6.667 (d, 3H, H6, H10, H9) 5.976 (bs, 1H, NHCO), 4.054-4.082 (m, 1H, CH), 3.859 (bs, 2H, H19), 3.787-3.822 (s, 6H, OCH_3), 3.457-3.552 (m, 2H, NCH_2), 2.731-2.770 (t, 2H, CH_2Ar), 2.530-2.573 (m, 2H, H18), 2.069 (s, 3H, SCH_3); ^{13}C {^{1}H} NMR (100 MHz, chloroform-d, δ ppm): 170.73 (C2), 167.26 (C11), 159.31 (C13), 149.30 (C7), 147.92 (C8), 133.33 (C15), 131.35 (C5), 130.88 (C17), 124.13 (C12), 120.74 (C16), 119.18 (C10), 118.82 (C14), 111.83 (C9), 111.43 (C6), 72.04 (C1), 55.94 (OCH_3), 55.94 (OCH_3), 40.69 (C3), 35.15 (C4), 32.83 (C18), 30.17 (C19) 15.13 (C20).

3b: Yield: 355 mg (90%); m.p. 80-81°C; Elemental Anal. calcd. (found) for $C_{22}H_{27}N_2O_4SBr$: C, 53.33 (53.35); H, 5.49 (5.52); N, 5.65 (5.69); UV-Vis (λ_{max} nm, ε $M^{-1}cm^{-1}$): 331, 436; FT-IR (ATR, ν cm^{-1}): 3316, 2931, 2842, 1648, 1629, 1541, 1516, 1473, 1235, 1139, 1025, 853, 822, 761, 671, 625, 541; UV-Visible (λ_{max} nm, ε $M^{-1}cm^{-1}$): 258 (24,398), 277 (20,756), 321 (6,390); ^{1}H NMR (399.82MHz, chloroform-d, δ ppm):12.298 (s, 1H, OH), 8.280 (s, 1H, CH=N), 7.421-7.481 (m, 2H, H14, H15), 6.902-6.922 (d, 1H, H17), 6.643-6.669 (d, 3H, H6, H10, H9), 5.932 (bs, 1H, NHCO), 4.066 (b, 1H, CH), 3.832 (b, 1H, H18), 3.798 (s, 6H, OCH_3), 3.517 (m, 2H, NCH_2), 2.758 (bs, 2H, H19), 2.548 (m, 1H, H18), 2.347 (m, 2H, CH_2Ar) 2.079(s, 3H, SCH_3); ^{13}C {^{1}H} NMR (100MHz, chloroform-d, δ ppm): 170.67 (C2), 167.11 (C11), 159.78 (C13), 149.31 (C7), 147.94 (C8), 136.09 (C15), 134.33 (C5), 130.88 (C17), 120.74 (C12), 119.80 (C16), 119.23 (C10), 111.88 (C14), 111.47 (C9), 110.90 (C6), 72.01 (C1), 55.96 (OCH_3), 55.96 (OCH_3), 40.67 (C3), 35.13 (C4), 32.84 (C18), 30.17 (C19) 15.12 (C20).

3c: Yield: 355 mg (90%); m.p. 80-81°C; Elemental Anal. calcd. (found) for $C_{22}H_{28}N_2O_4S$: C, 63.44 (63.40); H, 6.78 (6.73); N, 6.73 (6.75); FT-IR (ATR, ν cm^{-1}): 3346, 2932, 2830, 1664, 1624, 1511, 1461, 1249, 1139, 1084, 1026, 738, 637;UV-Visible (λ_{max} nm, ε $M^{-1}cm^{-1}$): 333, 432; ^{1}HNMR (399.82MHz, chloroform-d, δ ppm):12.751 (s, 1H, OH), 8.362 (s, 1H, CH=N), 7.001-7.019 (d, 1H, H5), 6.854-6.947 (m, 2H, H16, H17), 6.647-6.701 (m, 3H, H6, H9, H10), 6.103 (bs, 1H, NHCO), 4.061-4.091 (m, 1H, CH), 3.934 (s, 3H, OCH_3), 3.822 (d, 2H, H18), 3.787 (s, 3H, OCH_3), 3.752 (s, 3H, OCH_3) 3.416-3.564 (m, 2H, NCH_2), 2.586-2.758 (t, 2H, H4), 2.289-2.425 (m, 2H, H19), 2.031 (s, 1H, SCH_3); ^{13}C{^{1} H} NMR (100 MHz, chloroform-d, δ ppm): 171.05 (C2), 168.48 (C11), 150.87 (C13), 149.25 (C14) 148.46 (C7), 147.87 (C8), 131.05 (C16), 123.73 (C15), 120.89 (C17), 119.11 (C5), 118.46 (C12), 115.16 (C10), 111.69 (C9), 111.55 (C6), 71.94 (C1), 56.30 (OCH_3), 56.19 (OCH_3), 40.85 (C3), 35.35 (C4), 33.38 (C18), 30.09 (C19) 15.12 (C20).

2.3 Antimicrobial activity.

The antimicrobial interest of latest (3a-3c) ligands became screened via agar nicely diffusion method [15] in opposition to four microorganism by following the standard procedure of incubation [19,20] which have been maintained for each compound, and the not unusual values are advised and tabulated.

2.4 Molecular docking

Docking calculation was executed by using software's and the process as mentioned in [20] and binding strength calculation were expressed in the table.

3. Results and discussion

3.1 Synthesis

The compound, **2** has been synthesized as mentioned in the literature [16]. The Schiff bases (**3a-3c**) were obtained by the condensation of amide, **2** with diverse salicylaldehyde derivatives such as 5-chlorosalicylaldehyde, 5-bromosalicylaldehyde, and orthovanillin in equimolar ratio at room temperature the use of dry methanol as a solvent, as represented in **Scheme 1**. The Schiff's bases, **3a-3c** are easily soluble in $CHCl_3$, CH_2Cl_2, C_2H_5OH, CH_3OH, DMSO and DMF at room temperature. The structures of the synthesized compounds were presented in **Chart 1**.

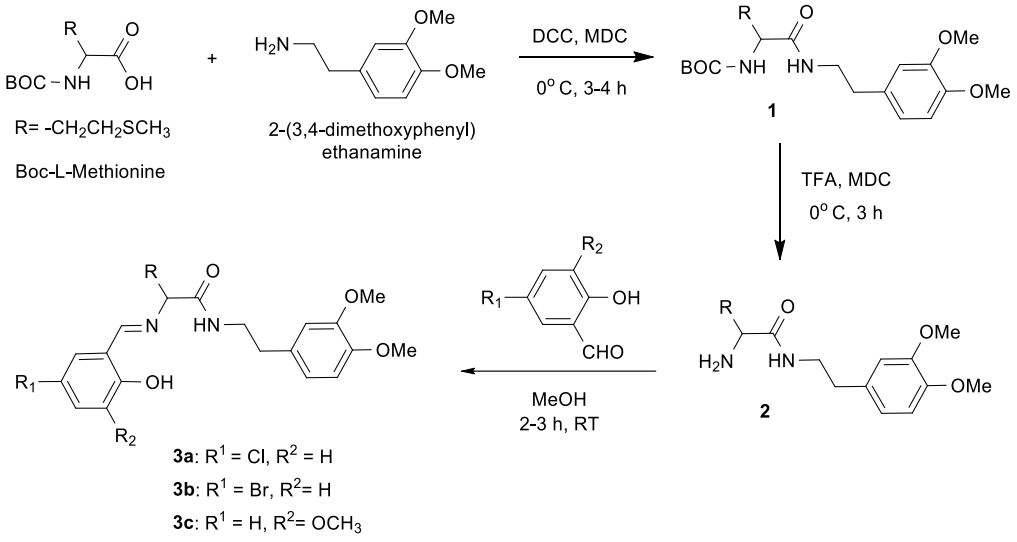

Scheme 1. Synthesis of **3a-3c**

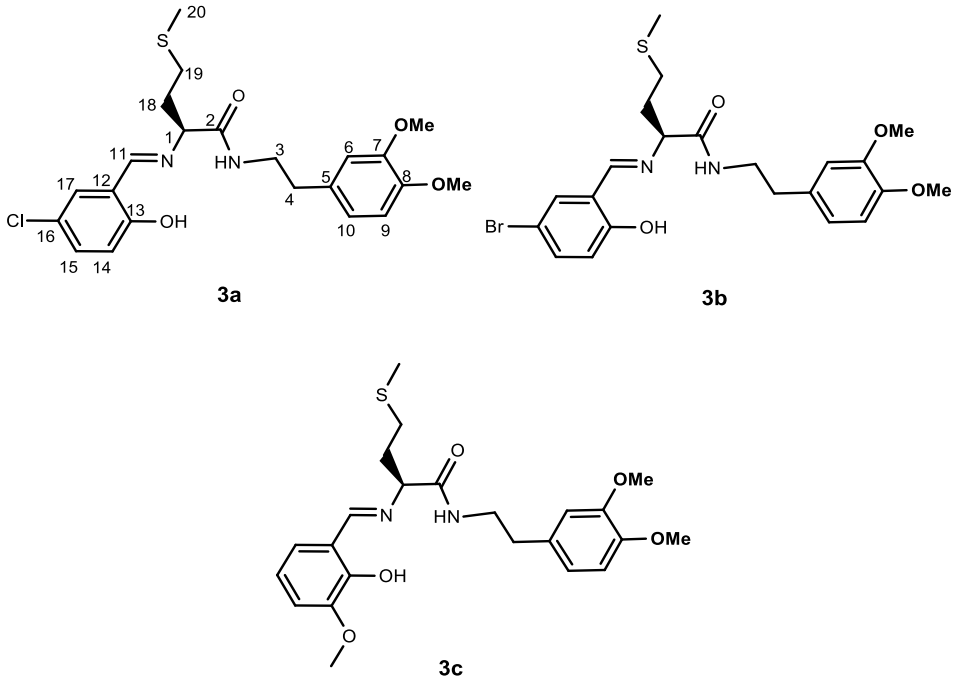

Chart 1. Structure of **3a-3c**

3.2 UV-Visible Spectroscopy

The UV-Visible spectra of **3a-3c** (2.5×10^{-5} M) have been recorded in DMSO solvent. The intense bands observed at around λmax 330 nm due to the n→π* and π→π* transitions in **3a-3c**. The weak bands between λmax, 430-435 nm were attributed to the charge transfer transitions within the delocalized sysyem. The combined UV-visible spectra of **3a-3c** are shown in **Fig. 1** [16].

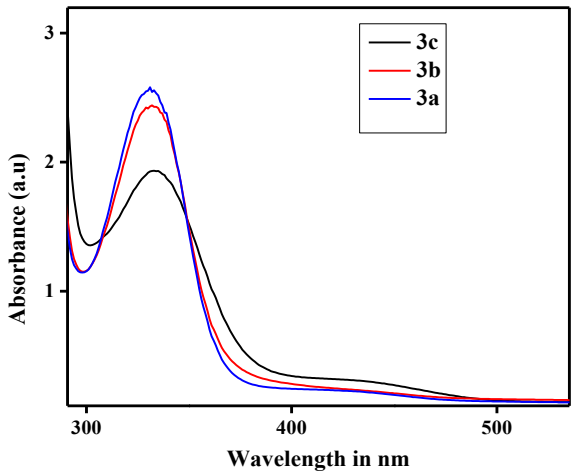

Fig. 1 UV-Visible spectra of **3a-3c**

3.3 FT-IR Spectroscopy

In **3a-3c** FT-IR spectra (**Fig. 2**), the N-H and imine -N=C< stretching vibrational bands appeared at ῡ, 3316-3346 cm^{-1} and 1625-1629 cm^{-1}. The amide CONH stretching bands are found between ῡ, 1645-1665 cm^{-1}. The bands displayed between ῡ, 1260-1235 cm^{-1} due to C-O stretching. [16]

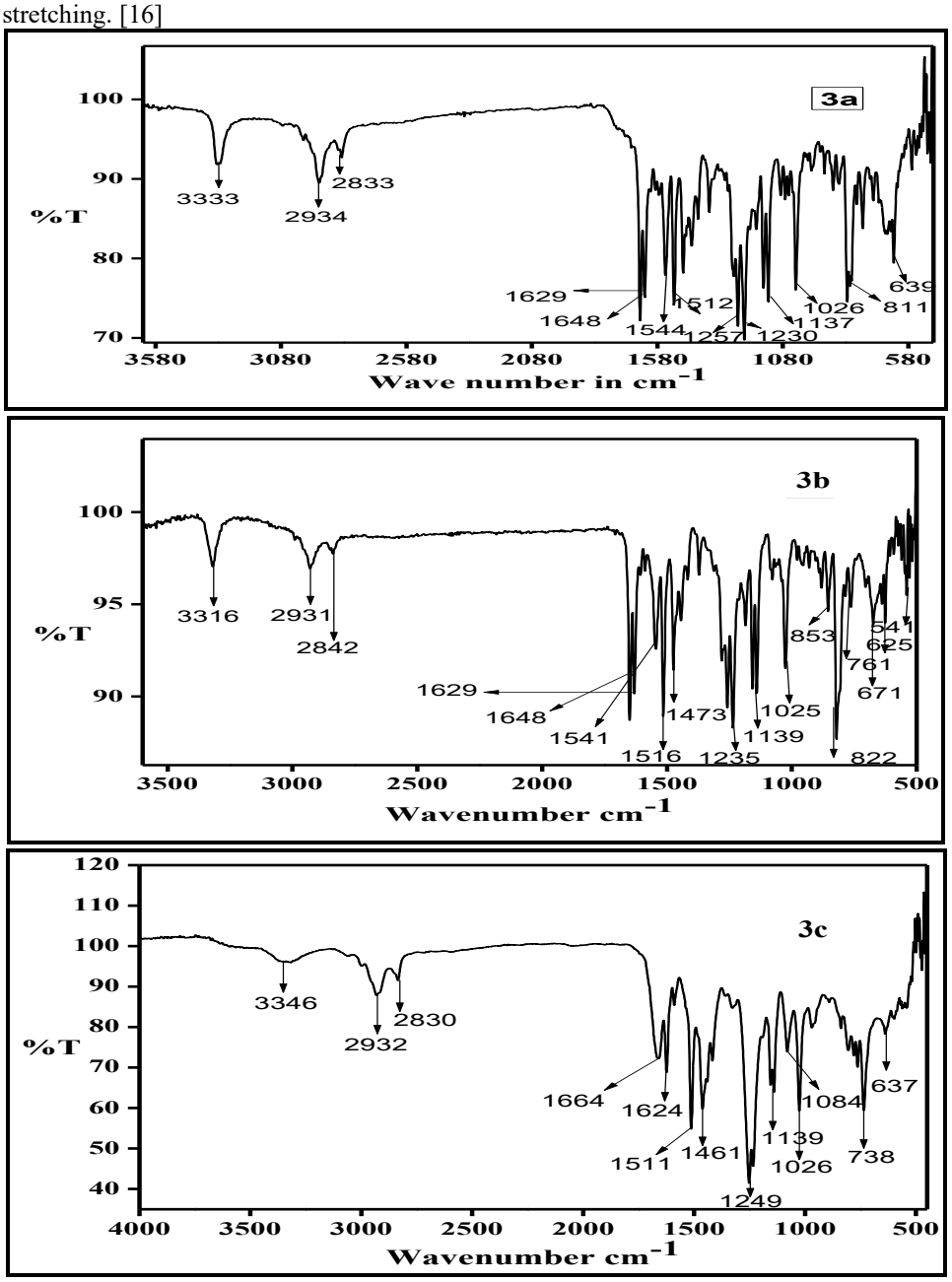

Fig. 2 FT-IR spectra of **3a-3c**

3.4 NMR Spectroscopy

In the **3a-3c** ^{1}H-NMR spectra (**Fig. 3**), the OH proton appeared at deshielded region of δ, ~12 ppm due to the Ar-O-H…N=C hydrogen bonding [22,23]. The Aryl-CH_2 and N-CH_2 protons found as triplets at δ 2.739-2.774 and 3.464-3.592 ppm, correspondingly. The signal for HC=N and >CO-NH proton appeared at δ, 7.90-8.35 ppm (as singlet) and ~6 ppm (triplet) respectively. The signals for other protons in **3a-3c** appeared at their characteristic δ ppm and the ^{1}H NMR spectra are characteristic with the structure of **3a-3c**.

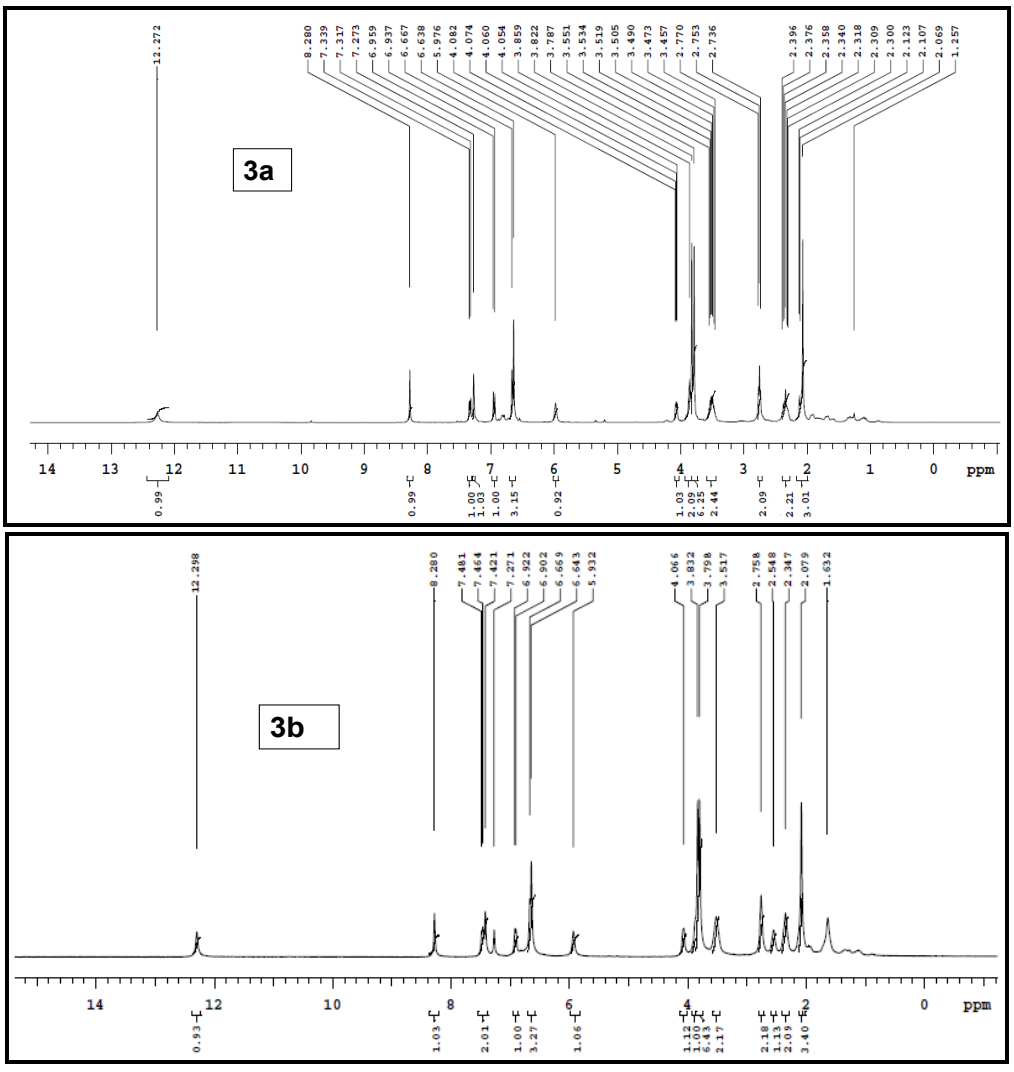

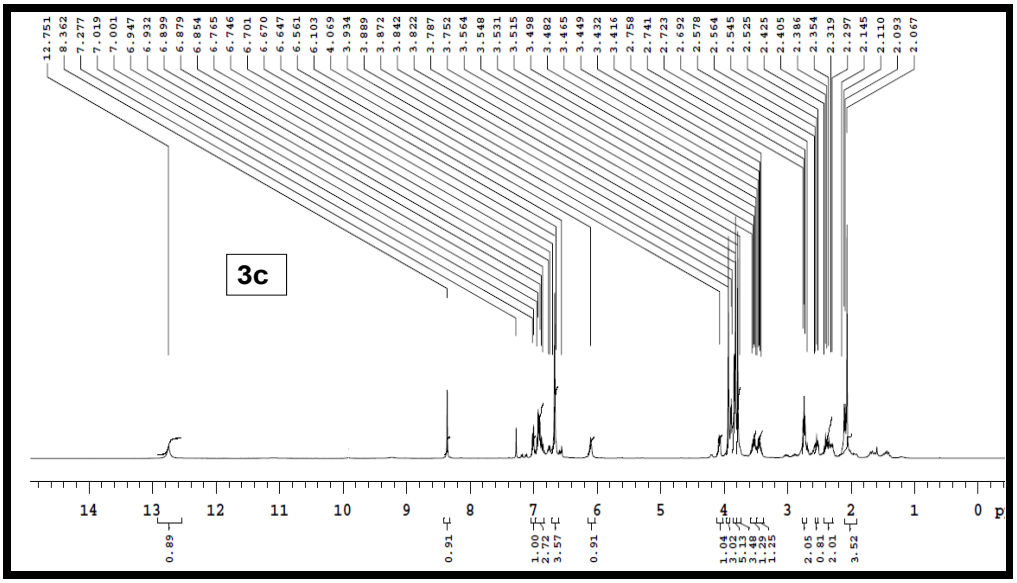

Fig. 3 ^{1}H-NMR spectrum of **3a-3c**

In the **3a-3c** ^{1}H-NMR spectra (**Fig. 4**), the $ArCH_2$ carbon peak found at δ, ~35 ppm, whereas the signal for N-CH_2 become observed particularly deshielded and observed at δ, ~40 ppm. In **3a-3c**, the carbon peaks for phenolic (ArC-OH) and >C=N- appeared at δ, 150-160 and ~168 ppm. The H^1 and ^{13}C-NMR spectral data correlate with the respective structure of **3a-3c**.

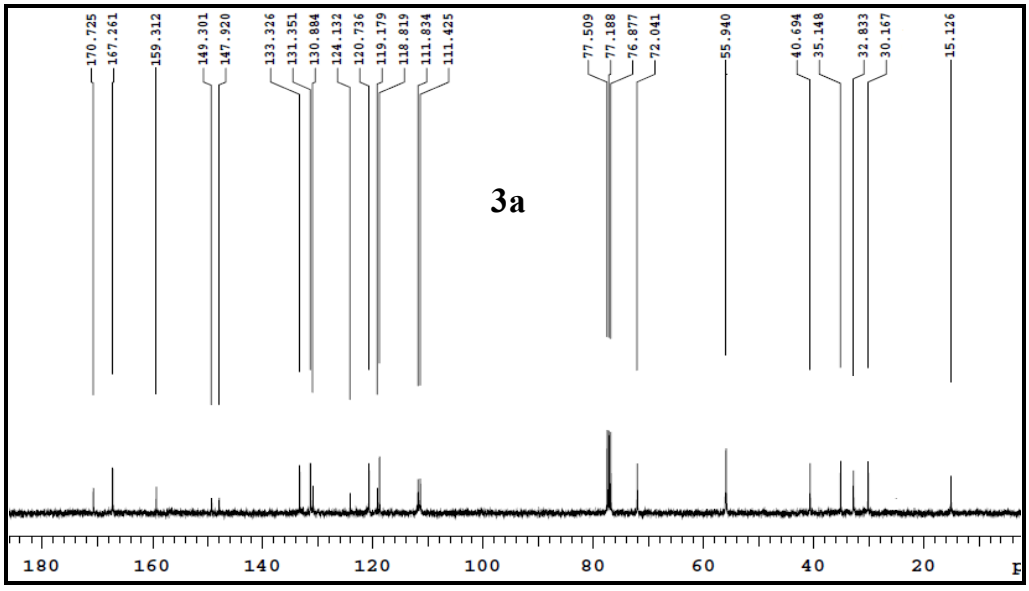

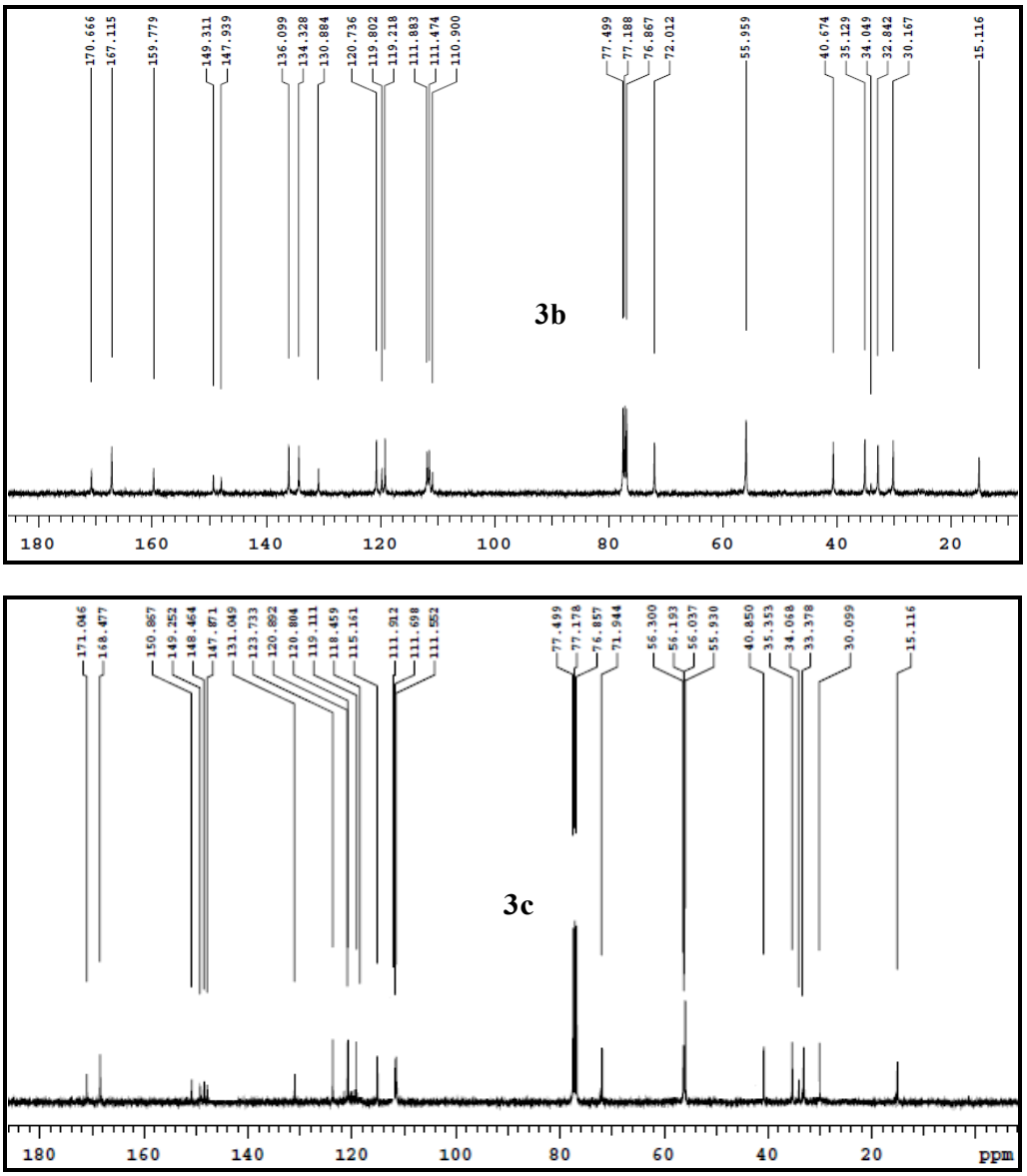

Fig. 4 ^{13}C {^{1}H} NMR spectrum of **3a-3c**

3.5 Cyclic voltammetry

The CV of **5a-5d** were studied as per the reported procedure [18]. The CV curves of **3a-3c** are shown in **Fig. 5**, the compounds **3a** (+1.049V) and **3b** (+1.049V) were showed one oxidation peak however **3c** showed two oxidation peaks (Eox, +0.976, +1.142V). The energy of HOMO and LUMO were determined based on oxidation potential and band gap respectively, corresponding to the onset wavelength ($\lambda_{max.}$) as shown in the **Table 1**.

Table 1 UV-Visible and CV data of 3a-3c

Compound	3a	3b	3c
λ_{max} (nm)	322.258	329.436	332.436
E_{ox} (V)	+1.224	+1.049	+0.976; +1.142
E_{red} (V)	-1.184	-1.222	-0.756
E_{HOMO} (eV)	-5.624	-5.449	-5.542
E_{LUMO} (eV)	-1.773	-1.692	-1.821
E_g (eV)	3.851	3.757	3.721

E_{HOMO} = - (E_{ox} (Fc/Fc$^+$) + 4.8) eV, Fc/Fc$^+$= 0.4; E_{LUMO}= E_{HOMO} + E_g; Band gap, E_g = 1240/$\lambda_{max.}$

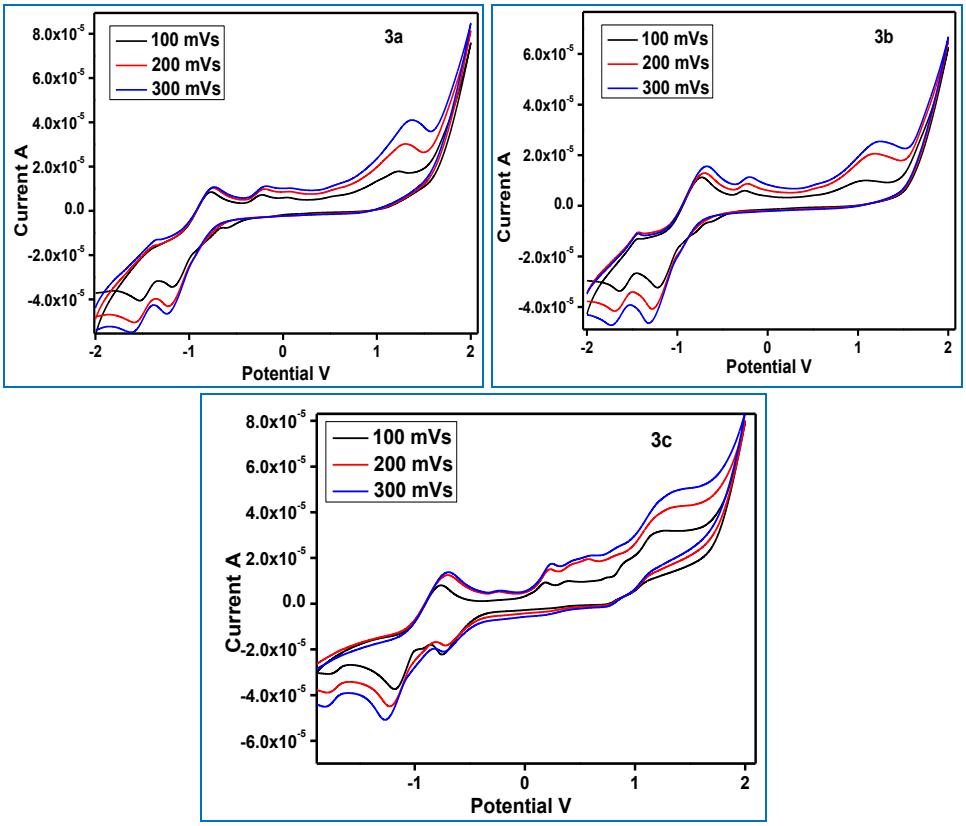

Fig. 5 Cyclic Voltammetry of **3a-3c** with scan rate of 100-300 mV/s

3.6 Antimicrobial activity and antifungal activity.

The antibacterial and antifungal activity data of **3a-3c** were tabulated in **Table 2** and **3**, and their graphical peaks are shown in **Fig. 6**. These observations indicated that the **3a-3c** have been shown significant antibacterial (in *P. desmolyticum* and *S. aureus*) and antifungal activity (in *A. flavus*) [19,20].

Table 2. Antibacterial activity of **3a-3c**

Sample	Treatment (μg/μL)	*K.aerogenes* (Mean ± SE)	*E. coli* (Mean ± SE)	*S. aureus* (Mean ± SE)	*P. desmolyticum* (Mean ± SE)
Cipro	5/50	14.67 ± 0.03	11.67 ± 0.05	15.00 ±0.03	13.67 ± 0.03
3a	500/50	1.30 ± 0.06	1.20 ± 0.07	1.15 ± 0.00	1.40 ± 0.00
	1000/100	2.30 ± 0.12	2.20 ± 0.07	2.25 ± 0.07	2.50 ± 0.06
3b	500/50	1.40 ± 0.00	1.30 ± 0.00	1.50 ± 0.00	1.90 ± 0.00
	1000/100	2.80 ± 0.00	2.90 ± 0.17	2.70 ± 0.17	3.10 ± 0.07
3c	500/50	1.70 ± 0.01	1.50 ± 0.06	1.80 ± 0.06	2.30 ± 0.00
	1000/100	3.20 ± 0.17	3.10 ± 0.03	3.40 ± 0.12	3.95 ± 0.00

Values are the mean ± SE of zone of inhibition in mm, Cipro: Ciprofloxacin

Table 3. Antifungal activity of **3a-3c**

Sample	Treatment (μg/μL)	*A. flavus* (Mean ± SE)	*C. albicans* (Mean ± SE)
Fluconazole	200/50	10.30 ± 0.03	11.60 ± 0.06
3a	250/25	1.60 ± 0.00	1.80 ± 0.03
	500/50	2.10 ± 0.33	2.30 ± 0.03
3b	250/25	1.50 ± 0.04	1.70 ± 0.00
	500/50	2.00 ± 0.00	2.20 ± 0.01
3c	250/25	1.60 ± 0.00	1.70 ± 0.06
	500/50	2.20± 0.03	2.30 ± 0.03

Values are the mean ± SE of zone of inhibition in mm

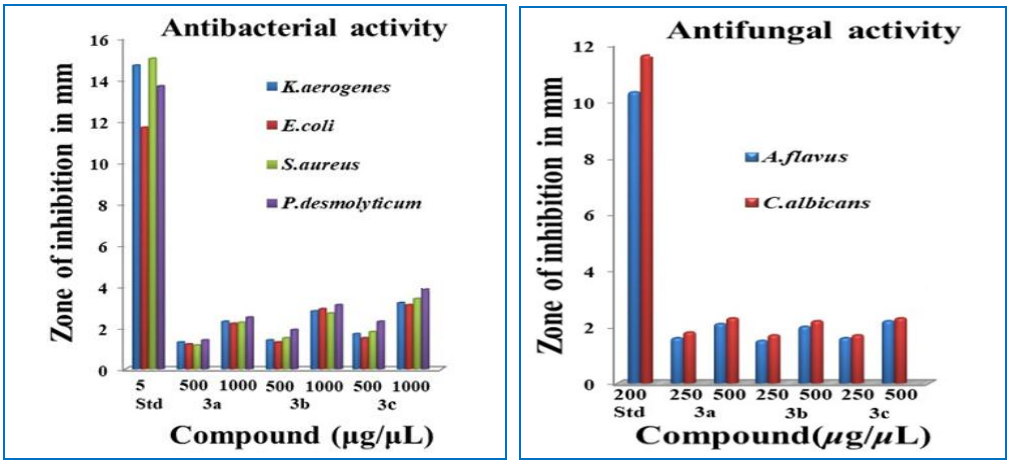

Fig. 6 Antibacterial activity and antifungal activity of **3a-3c**

3.7 *Insilico* studies

The **5a-5d** structures were drawn using Chemdraw and optimization was achieved as per the reported method. The refined molecules of ligands and protein docked using DS 3.5. The interaction modes between the **3a-3c** and protein were studied using Biosolve IT FlexX. The results of the docking study are tabulated in **Table 4** and **5**. [21,22]

Table 4. Docking results of compounds against 3G75 target

Comp.	Pose	Binding Energy (delta G)	No. of interactions	H bonding
3a	7	-7.59	2	Tyr-335, His-227
3b	9	-6.07	3	His-227, Tyr-225, Tyr-354
3c	6	-6.46	4	Leu-451, Tyr-225, Tyr-354, Tyr-335

The docking of **3a-3c** into the active site of target protein 3G75 and 1IYL resulted the binding energy in between -6.07 to -7.59 and -8.9 to -10.2 kcal/mol. All the compounds are involved in the hydrogen bonding with target. The binding mode compounds with target protein DNA gyrase and N-myristylsynthase transferase are given in **Fig. 7** and **8**.

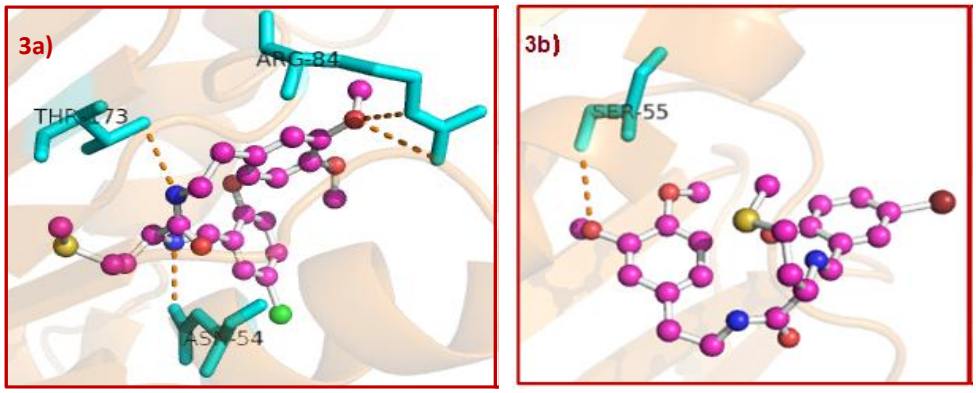

Fig. 7 Binding pose of **3a-b** with DNA gyrase target

Table 5 Docking results of compounds against 1IYL target

Comp.	Pose	Binding Energy (delta G)	No. of Interactions	H bonding
3a	7	-9.09	2	Try-335, His-227
3b	3	-10.2	3	His-227, Tyr-225, Tyr-354
3c	9	-8.9	4	Tyr-225, Tyr-354, Tyr-335, Leu-451

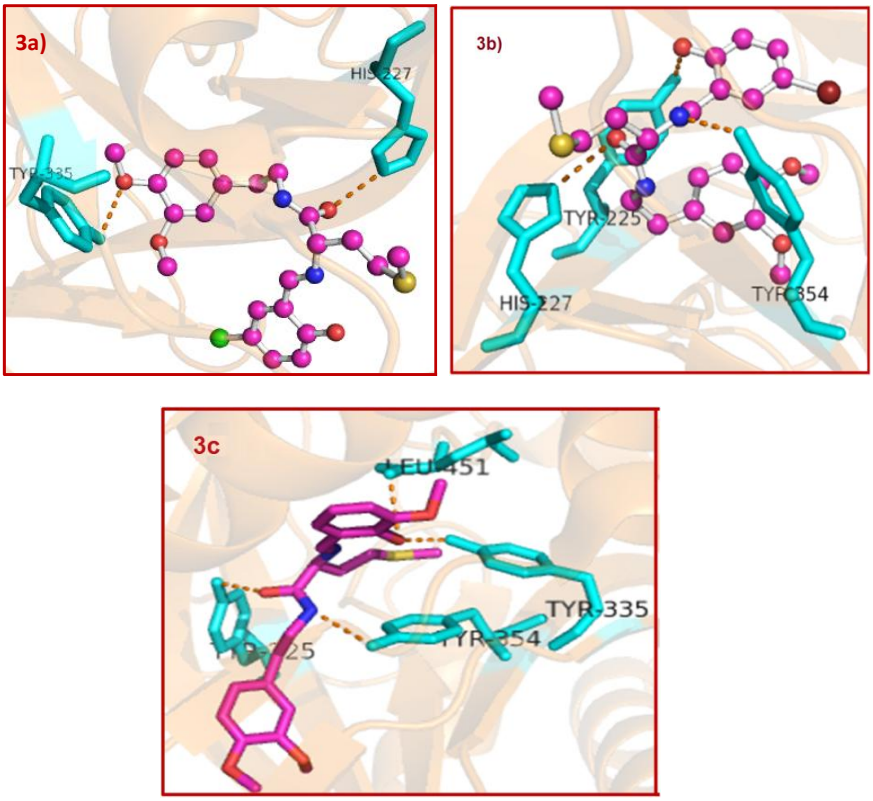

Fig. 8 Binding pose of **3a-3c** with N-myristylsynthase transferase

4. Conclusion

A new L-methionine-primarily based Schiff base compound, **3a-3c**, has been synthesized done condensation among L-2-amino-N-(three,four-dimethoxyphenethyl)-four-(methylthio)butanamide (2) and salicylaldehyde derivatives. The synthesized **3a-3c** compounds were characterized by feet-IR, UV–Vis. CV, ^{1}H- and ^{13}C{^{1}H}-NMR spectroscopy. Molecular docking studies of compounds 3a and 3c validated their effective binding inside the energetic website of the target protein, with binding energies ranging from -6.07 to -7.59 kcal/mol. substantially, docking against the fungal goal protein confirmed the binding affinity, with energies between -8.9.and -10.2 kcal/mol. all the compounds are worried inside the hydrogen bonding with the goal. All the compounds **3a–3c** show off hydrogen bonding interactions with the goal.

References

[1] Vale, N., Ferreira, A., Matos, J., Fresco, P., & Gouveia, M. J.: Amino acids in the development of prodrugs. Molecules, 23(9), 2318(2018)

[2] Eranna, S. C., Panchangam, R. K., Kengaiah, J., Adimule, S. P., Foro, S., & Sannagangaiah, D.: Synthesis, structural characterization, and evaluation of new peptidomimetic Schiff bases as potential antithrombotic agents. Monatshefte Für Chemie - Chemical Monthly, 153(7–8), 635–650(2022)

[3] Hanessian, S., McNaughton-Smith, G., Lombart, H., & Lubell, W. D.: Design and synthesis of conformationally constrained amino acids as versatile scaffolds and peptide mimetics. Tetrahedron, 53(38), 12789–12854(1997)

[4] Mann, E., Chana, A., Sánchez-Sancho, F., Puerta, C., García-Merino, A., & Herradón, B.: Novel Peptide-Heterocycle hybrids: Synthesis and preliminary studies on Calpain inhibition.AdvancedSynthesis &Catalysis,344(8),pp.855–867(2002)

[5] Schmidt, G.:Recent developments in the field of biologically active peptides. In Topics in current chemistry. pp. 109–159(1986)

[6] Saitton, S., Del Tredici, A. L., Mohell, N., Vollinga, R. C., Boström, D., Kihlberg, J., & Luthman, K.: Design, synthesis and evaluation of a PLG tripeptidomimetic based on a pyridine scaffold. Journal of Medicinal Chemistry, 47(26), pp.6595–6602(2004)

[7] Lu,Y.:Design and engineering of metalloproteins containing unnatural amino acids or non-native metal-containing cofactors. Curr. Opin. Chem. Biol.9(2), pp.118–126(2005)

[8] Giannis, A., Rubsam, F.:Peptidomimetics in Drug Design. Adv. Drug Res.29,pp.1-78(1997)

[9] Ripka, A. S., & Rich, D. H.: Peptidomimetic design. Current Opinion in Chemical Biology. 2(4), 441–452 (1998)

[10] Gluck, M. R., & Zeevalk, G. D.: Inhibition of brain mitochondrial respiration by dopamine and its metabolites: implications for Parkinson's disease and catecholamine associated diseases. Journal of Neurochemistry, 91(4), 788–795(2004)

[11] Venkatachalam, G., & Ramesh, R.: Catalytic and biological activities of Ru(III) mixed ligand complexes containing N,O donor of 2-hydroxy-1-naphthylideneimines. Spectrochimica Acta Part a Molecular and Biomolecular Spectroscopy, 61(9), pp.2081–2087(2004)

[12] Singh, B. K., Jetley, U. K., Sharma, R. K., & Garg, B. S.: Synthesis, characterization and biological activity of complexes of 2-hydroxy-3,5-dimethylacetophenoneoxime (HDMAOX) with copper(II), cobalt(II), nickel(II) and palladium(II). Spectrochimica Acta Part a Molecular and Biomolecular Spectroscopy, 68(1), pp.63–73(2006)

[13] Daniel, V. P., Murukan, B., Kumari, B. S., & Mohanan, K.: Synthesis, spectroscopic characterization, electrochemical behaviour, reactivity and antibacterial activity of some transition metal complexes with 2-(N-salicylideneamino)-3-carboxyethyl-4, 5-dimethylthiophene. Spectrochimica Acta Part A: Molecular and Biomolecular Spectroscopy. 70(2), pp.403-410(2008)

[14] Corey, E. J., & Link, J. O.: A catalytic enantioselective synthesis of denopamine, a useful drug for congestive heart failure. The Journal of Organic Chemistry, 56(1), pp.442–444(1991)

[15] Ramesh, G., Kumar, N. S., Kumar, P. R., Suchetan, P., Devaraja, S., Sabine, F., & Nagaraju, G.: Synthesis, characterisation, crystal structures, anticoagulant and antiplatelet activity studies of new 2,6-dipyrazinylpyridines with pendant trimethoxyphenyl. Journal of Molecular Structure, 1200, 127040(2019).

[16] Satheesh C. E., Raghavendra Kumar P., Jayanna K., Suchetan P. A., Sabine Foro & Devaraju S. Synthesis, structural characterization, and evaluation of new peptidomimetic Schiff bases as potential antithrombotic agents, Monatsh Chem. 153(7-8):635–650 (2022). doi: 10.1007/s00706-022-02936-6

[17] Krishnaswamy G., Desai Nivedita R., Raja Naika H., Sreenivasa S. and Aruna Kumar D.B.: Synthesis of novel 5-(4-N-Alkyl-piperazin-1-yl)-1- benzofuran-2-yl)-3-substituted phenyl propenone derivatives as antibacterial agents: In vitro and In silico studies. Research Journal of Chemistry and Environment. Vol. 27 (1), 78-85 (2023)

[18] Golla, R., Kumar, P. R., Suchethan, P., Foro, S., & Nagaraju, G.: Synthesis, photophysical, electrochemical properties and crystal structures and Hirschfeld surface analysis of 4′-dimethoxyphenyl-(2,6-di-2-pyrazinyl) pyridines. Journal of Molecular Structure, 1201, 127118(2019)

[19] Dong, X., Li, Y., Li, Z., Cui, Y., & Zhu, H. Synthesis, structures and urease inhibition studies of copper(II) and nickel(II) complexes with bidentate N,O-donor Schiff base ligands. Journal of Inorganic Biochemistry. 108, pp.22–29(2011)

[20] Satheesh, C. E., Kumar, P. R., Sharma, P., Lingaraju, K., Palakshamurthy, B. S., & Naika, H. R.: Synthesis, characterisation and antimicrobial activity of new palladium and nickel complexes containing Schiff bases. Inorganica Chimica Acta. 442, pp.1-9(2016)

[21] Shivaraja G., Sanay N., T. Madhuchakrapani R., B.C. Revanasiddappa, S. M. Srinivasa, L. Parashuram, Sivan Velmathi, S. Sreenivasa: Sulfated magnesium zirconate catalyzed synthesis, antimicrobial, antioxidant, anti-inflammatory, and anticancer activity of benzo[*d*]thiazole-hydrazone analogues and its molecular docking. Results in Chemistry. 3 , 100197 (2021)

[22] Krishnaswamy G., Desai Nivedita R., Raja Naika H., Sreenivasa S. and Aruna Kumar D.B.: Synthesis of novel 5-(4-N-Alkyl-piperazin-1-yl)-1- benzofuran-2-yl)-3-substituted phenyl propenone derivatives as antibacterial agents: In vitro and In silico studies. Research Journal of Chemistry and Environment. Vol. 27 (1), 78-85 (2023)